

# RESONANT PRESSURE SENSING USING A MICROMECHANICAL CANTILEVER ACTUATED BY FRINGING ELECTROSTATIC FIELDS

Naftaly Krakover<sup>1</sup>, B. Robert Ilic<sup>2</sup>, and Slava Krylov<sup>1</sup>

<sup>1</sup>The School of Mechanical Engineering, Faculty of Engineering, Tel Aviv University, Ramat Aviv 69978, Tel Aviv, ISRAEL

<sup>2</sup>Center for Nanoscale Science and Technology, National Institute of Standards and Technology, Gaithersburg, MD, 20899, USA

## ABSTRACT

We demonstrate a pressure-sensing approach based on the resonant operation of a single-crystal Si cantilever positioned near a flexible, pressurized membrane. The membrane deflection perturbs the electrostatic force acting on the cantilever and consequently alters the beam's resonant frequency. Sensitivity was enhanced by tailoring the actuating force nonlinearities through fringing electrostatic fields. With our coupled micromechanical system, we achieved frequency sensitivity to pressure and displacement of  $\approx 30$  Hz/kPa and  $\approx 4$  Hz/nm, respectively. Our results indicate that the suggested approach may have applications not only for pressure measurements, but also in a broad range of microelectromechanical resonant inertial, force, mass and bio sensors.

## INTRODUCTION

Resonant micromechanical sensors are based on monitoring the spectral characteristics of a structure rather than static structural displacements [1]. In resonant pressure sensors, the common interrogation technique is based on a vibrating wire anchored, at its ends, to a flexible pressure-driven membrane. Deflection of the membrane results in stretching of the wire and modulation of its natural frequency [2]. In these devices, either complex force amplification mechanisms [2] or extreme dimensional downscaling [3], which may complicate fabrication, are necessary to overcome the high tensile stiffness of the vibrating wire and to improve sensitivity. Moreover, frequency of doubly-clamped wires is affected by residual and thermal stresses.

Micro- and nano-scale devices incorporating cantilevers as the sensing elements have numerous applications in diverse fields ranging from engineering to life and physical sciences. These sensors are used for the detection of small masses, biomolecular binding events, and non-contact topographic and localized charge imaging using atomic force microscopy [4]. The key advantage of cantilever-based devices are their lower (when compared to doubly-clamped beams and wires) stiffness and reduced sensitivity to temperature and residual stress.

Despite their widespread use, vibrating cantilevers have not yet been implemented in resonant pressure sensors. A cantilever sensor exploiting the effect of ambient pressure on the frequency of a resonator was reported in [5]. Cantilevers were placed in an evacuated chamber and resonant frequencies were measured at values of pressure varying between 0.1 Pa to  $10^5$  Pa. The use of this kind of device for open-air pressure

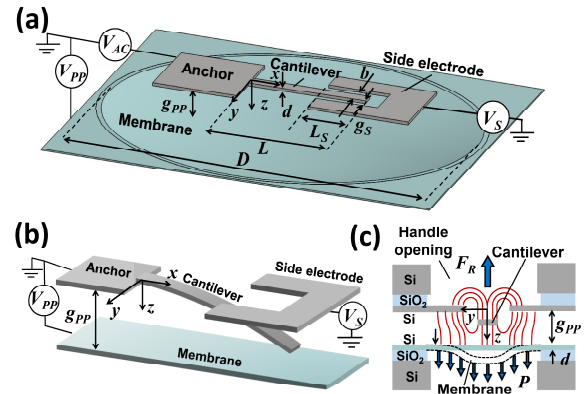


Figure 1: Schematic illustration of the device. (a) The cantilever is positioned above a pressure-driven, deformable membrane. The handle wafer that the cantilever is attached to is not shown. (b) Deformed cantilever is actuated by the parallel plate PP and side electrodes. (c) Device cross section showing the cantilever, the side electrode and the membrane. The restoring force  $F_R$  appears due to the asymmetry of the fringing fields (thin red lines). Dashed line shows the deformed membrane.

measurements could be challenging since the cantilever response is also influenced by other factors such as temperature, humidity and contamination. In the present work, we introduce a membrane-based pressure sensor, which incorporates an oscillating cantilever as the sensing element. To ensure controlled environmental conditions, the cantilever can be positioned in a sealed cavity under the membrane, whereas the other side of the membrane is exposed to ambient conditions.

Significant research efforts have been devoted to design and measurement method improvements, as reviewed in [4]. The most commonly explored sensing scenarios primarily focus on the linear operating regimes of the vibrating structure. One of the emerging strategies for sensitivity enhancement is based on device operation in a nonlinear regime. In these structures, especially when actuation takes place near instability points, small variations in the detection parameter may lead to a large response changes, therefore improving sensitivity [6-9]. Electrostatically actuated devices manifest the so-called pull-in instability associated with the nonlinearity of the actuating forces. Operation near the pull-in point, where the effective device stiffness is minimal due to the electrostatic softening, increases frequency sensitivity [7]. However, operation near the instability has drawbacks

including a possibility of device collapse into the electrode and irreversible damage.

An alternative approach for sensitivity enhancement of cantilever-type architectures operating near critical points is based on the actuation by fringing electrostatic fields [10]. This kind of actuation introduces an additional nonlinearity that can lead to an inflection point in the voltage-deflection dependence, where the cantilever is on the verge of bistability. It was shown theoretically [10] that device operation near the critical point may lead to sensitivity enhancement by more than an order of magnitude.

In this work, we present a pressure sensor based on a cantilever-near-a-membrane type resonant device. To enhance sensitivity, the cantilever is actuated near an inflection point by the electrostatic fringing fields and the parallel-plate capacitive forces. The suggested actuation mechanism can be used as a general approach for other displacement sensing devices.

## DEVICE ARCHITECTURE AND OPERATIONAL PRINCIPLE

The device die, containing a cantilever of length  $L$ , width  $b$ , and thickness  $d$ , is attached to the flexible membrane of diameter  $D$ . The initial distance between the cantilever and the membrane, defining the gap within the parallel plate (PP) capacitive actuator, is  $g_{PP}$  (Fig. 1). The planar side (S) electrode of length  $L_S$ , located at a distance  $g_S$  from the cantilever (Fig. 1a), is a source of the restoring electrostatic force  $F_R$  associated with the fringing fields [10] (Fig 1c). A pressure  $P$  causes the membrane to deflect. This leads to an increase of the gap  $g_{PP}$  between the membrane and the cantilever.

In general, the electrostatic force acting on the beam is affected by the interaction between the S and the PP electrodes [10] and is more complicated than just a superposition of the forces. To model the effects, we first considered a case without a PP electrode, when the interaction is solely between the cantilever and the side electrode. The force  $f_s$  (per unit length of the beam) provided by the side electrode can be approximated by the expression [11]

$$f_s(x,t) = -\frac{\alpha\sigma(w/d)V_S^2}{1+\sigma|w/d|^\gamma} \quad (L_S \leq x \leq L) \quad (1)$$

where  $w(x,t)$  is the deflection of the beam,  $x$  and  $t$  are the coordinate along the beam and time, respectively,  $V_S$  is the voltage on the side electrode and  $\alpha$ ,  $\sigma$ ,  $\gamma$  are fitting parameters. Due to symmetry, the resultant electrostatic force is zero in the initial configuration. In the deflected state, the distributed electrostatic force, arising from asymmetries of the fringing fields, acts in a direction opposite to the beam's deflection and effectively serves as a restoring force [11]. In contrast, the nonlinear force provided by the parallel plate electrode, which can be approximated by the simplest PP capacitor formula,

$$f_{PP}(x,t) = \frac{\varepsilon_0 b V_{PP}^2}{2(g_{PP} - w)^2} \quad (2)$$

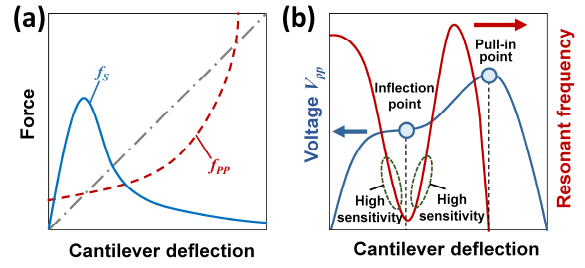


Figure 2: (a) Schematics of the mechanical (dash-dot line), electrostatic restoring forces  $f_s$  (solid line) and the electrostatic force  $f_{PP}$  (dashed line) as a function of the cantilever's deflection. (b) Resulting equilibrium curve (blue) and the resonant frequency of the beam (red) as a function of the beam's deflection.

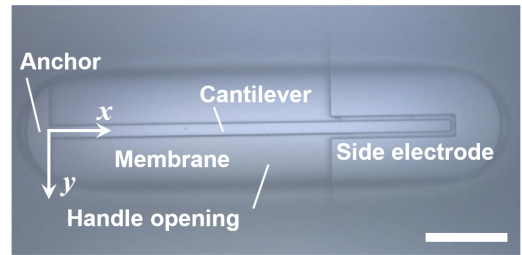


Figure 3: Optical micrograph of the integrated device. The image of the cantilever and of the side electrode is acquired through the opening in the handle wafer. Scale bar size is  $\approx 100 \mu\text{m}$ .

is of a divergent nature and consequently pulls the beam further away from its initial configuration. Here,  $\varepsilon_0$  is the dielectric permittivity and  $V_{PP}$  is the voltage applied to the PP electrode. The force  $f_{PP}$  is affected by the gap between the cantilever and the membrane, and therefore by the membrane deflection. Figure 2a shows schematically the qualitative dependence of the elastic, side force  $f_s$  and PP forces  $f_{PP}$  as a function of the beam's deflection (at  $x = L$ ). An equilibrium curve for a specific value of  $V_S$ , is shown in Fig 2b. The value of  $V_S$  can be chosen in such a way that the force-deflection curve contains an inflection point. In the vicinity of this point, both the effective stiffness and the frequency decrease, whereas the slope of the frequency-deflection curve (red line in Fig. 2b) becomes steeper. Changes in pressure  $P$  modify the gap  $g_{PP}$  and affect the natural frequency of the beam. By choosing appropriate  $V_S$  and  $V_{PP}$  such that the beam is positioned near the inflection point, frequency sensitivity of the beam to the membrane deflection can be significantly improved. We emphasize that Eqs. (1) and (2) are used here only to show a qualitative dependence between the frequency and the membrane deflection and to clarify the sensor's operational principle. Numerical approaches should be used for more accurate evaluation of this force [10,11].

## EXPERIMENT

Using deep reactive ion etching (DRIE), cantilevers, side electrodes and the membrane were fabricated from a  $\approx 5 \mu\text{m}$  thick, single crystal, silicon device layer using a silicon-on-insulator (SOI) wafer with a  $\approx 2 \mu\text{m}$  thick buried silicon dioxide layer. DRIE was also used to etch a cavity within the handle wafer to form the membrane and an opening in the handle under the cantilever to allow for large amplitude vibrations of the beam. Using a polymer spacer of thickness  $g_{PP}$ , the cantilever die was flipped upside down and attached to the membrane, in such a way that the device is facing the membrane, Fig 1c. Figure 3 shows an optical micrograph of the fabricated device with the dimensions  $L \approx 1000 \mu\text{m}$ ,  $b \approx 16 \mu\text{m}$ ,  $d \approx 5 \mu\text{m}$ ,  $g_S \approx 5 \mu\text{m}$ ,  $L_S \approx 5 \mu\text{m}$ ,  $g_{PP} \approx 10 \mu\text{m}$ , and  $D \approx 2000 \mu\text{m}$ . The experimental setup is presented in Fig. 4.

The assembly containing both chips, each with an approximate extent of  $1 \text{ cm} \times 1 \text{ cm}$ , were mounted onto a custom built printed circuit board (PCB). The beam and the side electrode were wire-bonded to the PCB contact pads. The double chip and the PCB stack assembly were placed onto a holder in such a manner that the membrane was positioned above a sink hole. The hole was connected by a tube to a pump applying a suction pressure in the range of  $P \approx 12 \text{ kPa}$  to  $P \approx 82 \text{ kPa}$ . The cantilever side of the membrane was at the atmospheric pressure.

The sinusoidal, zero offset, voltage signal with an amplitude of  $V_{AC} \approx 2 \text{ V}$ , provided by a network analyzer, was supplied to the cantilever. The frequency was swept between  $\approx 29 \text{ kHz}$  and  $\approx 34 \text{ kHz}$ . In addition, using a separate power supply, steady-state voltages  $V_{PP}$  and  $V_S$  were applied to the membrane and the side electrodes, respectively. Using a single-beam laser Doppler vibrometer (LDV) operated in a velocity acquisition mode, the out-of-plane response of the cantilever was measured. The positioning of the LDV laser spot was monitored by a camera mounted on the microscope. The output of the LDV was fed back into the network analyzer. In parallel to the spectral analysis of the output signal, the velocity time history of the LDV output was monitored with an oscilloscope.

An example of frequency response for  $V_S \approx 50 \text{ V}$ ,

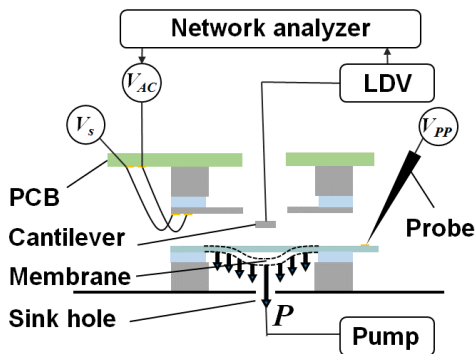


Fig. 4. Schematic illustration of the experimental setup. The device stack contains two SOI chips positioned on a PCB board, placed in such a way that the membrane is positioned above the sink hole. Cantilever vibrations were measured using the LDV through an opening in the handle of the SOI wafer and the PCB. Spectral response was measured using a network analyzer.

$V_{PP} \approx 30 \text{ V}$  and a varying pressure  $P$  is shown in Fig. 5. The measured spectra show a resonant frequency increase with increasing pressure. The experiments were carried out under various combinations of  $V_S$  and  $V_{PP}$ . Fig. 6a shows the resonant frequency  $f$  dependence on  $P$  for  $V_{PP} \approx 30 \text{ V}$  and  $V_{PP} \approx 70 \text{ V}$ . The slope  $df/dP$  of the curves represents the frequency sensitivity to pressure, as shown in the Fig. 6a inset. We found that higher sensitivity is reached for lower pressure values. This corresponds to a smaller gap  $g_{PP}$  and consequently larger PP capacitive force. In our experiments, we measured a sensitivity of

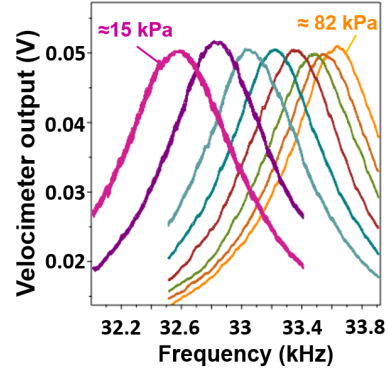


Fig 5. Measured resonant curves of the cantilever beam at a varying  $P$  for  $V_S \approx 50 \text{ V}$  and  $V_{PP} \approx 30 \text{ V}$ .

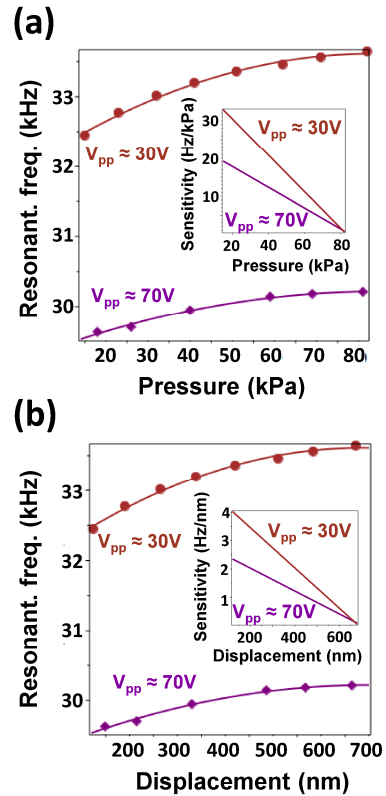


Fig. 6. (a) Resonant frequency as a function of the applied pressure at two values of  $V_{PP}$ . The slope of the response curve represents frequency sensitivity to pressure (inset). The one standard deviation frequency uncertainty based on a Lorentzian fit is smaller than the data marker size. (b) Resonant frequency as a function of membrane displacement and the corresponding frequency sensitivities to displacement (inset).

$\approx 30$  Hz/kPa of suction pressure under the membrane. This result is comparable to state-of-the-art values reported in the literature [2,12].

The suggested approach can be considered as a particular case of a generic displacement sensing method. In order to estimate the measured frequency sensitivity to the PP electrode displacement, membrane midpoint deflection  $w_0$  was calculated using the expression [13]

$$w_0 = \frac{3PD^4(1-\nu^2)}{256Ed^3 \left(1 + \frac{0.488w_0^2}{d^2}\right)} \quad (3)$$

Here,  $E$  and  $\nu$  are Young's modulus and the Poisson's ratio of the membrane material, respectively. By calculating the deflection for each value of  $P$  that the frequency was measured for, frequency sensitivity (scale factor) curves were obtained (Fig 6b). The highest measured frequency sensitivity-to-displacement was  $\approx 4$  Hz/nm.

## CONCLUSION

We demonstrate a cantilever-membrane resonant pressure sensing approach. Deflection of a membrane, resulting from pressure differences on its two sides, changes the nonlinear electrostatic force acting on the cantilever and consequently alters the cantilever's natural frequency. The use of the fringing electrostatic field actuation, in addition to the force provided by the parallel-plate actuator, allowed for tailoring of the effective nonlinearity of the system that in turn enhanced sensitivity. Along with pressure sensing, the suggested design can be used as a general approach to frequency-based displacement sensing. Our results indicate that the integrated sensing platform based on a coupled mechanical system may be applicable for a wide range of displacement sensing applications, ranging from pressure sensors and accelerometers to flow, tactile, inertial and precision force sensors.

## ACKNOWLEDGEMENTS

The devices were fabricated and tested at the Center for Nanoscale Science & Technology (CNST) at the National Institute of Standards and Technology (NIST) and at the Microsystems Design and Characterization Laboratory at Tel Aviv University.

## REFERENCES

- [1] R. Abdolvand, B. Bahreyni, J. Lee, and F. Nabki, "Micromachined Resonators: A Review," *Micromachines*, vol. 7, no. 9, p. 160, Sep. 2016.
- [2] X. Du, L. Wang, A. Li, L. Wang, and D. Sun, "High Accuracy Resonant Pressure Sensor With Balanced-Mass DETF Resonator and Twinborn Diaphragms," *J. Microelectromech. Syst.*, vol. 26, no. 1, pp. 235–245, Feb. 2017.
- [3] M. Messina, J. Njuguna, V. Dariol, C. Pace, and G. Angeletti, "Design and Simulation of a Novel Biomechanic Piezoresistive Sensor With Silicon Nanowires," *IEEE/ASME Trans. Mechatronics*, vol. 18, no. 3, pp. 1201–1210, Jun. 2013.
- [4] A. Boisen, S. Dohn, S. S. Keller, S. Schmid, and M. Tenje, "Cantilever-like micromechanical sensors," *Reports Prog. Phys.*, vol. 74, no. 3, p. 36101, 2011.
- [5] S. Bianco, M. Cocuzza, S. Ferrero, E. Giuri, G. Piacenza, C. F. Pirri, A. Ricci, L. Scaltrito, D. Bich, A. Merialdo, P. Schina, and R. Correale, "Silicon resonant microcantilevers for absolute pressure measurement," *J. Vac. Sci. Technol. B.*, vol. 24, no. 4, p. 1803, 2006.
- [6] N. Krakover, B. R. Ilic, and S. Krylov, "Displacement sensing based on resonant frequency monitoring of electrostatically actuated curved micro beams," *J. Micromech. Microeng.*, vol. 26, no. 11, p. 115006, Nov. 2016.
- [7] C. Comi, A. Corigliano, A. Ghisi, and S. Zerbini, "A resonant micro accelerometer based on electrostatic stiffness variation," *Meccanica*, vol. 48, no. 8, pp. 1893–1900, 2013.
- [8] A. Ramini, M. I. Younis, and Q. T. Su, "A low-g electrostatically actuated resonant switch," *Smart Mater. Struct.*, vol. 22, no. 2, p. 25006, Feb. 2013.
- [9] M. E. Khater, M. Al-Ghamdi, S. Park, K. M. E. Stewart, E. M. Abdel-Rahman, A. Penlidis, A. H. Nayfeh, A. K. S. Abdel-Aziz, and M. Basha, "Binary MEMS gas sensors," *J. Micromech. Microeng.*, vol. 24, no. 6, p. 65007, Jun. 2014.
- [10] N. Krakover and S. Krylov, "Bistable Cantilevers Actuated by Fringing Electrostatic Fields," *J. Vib. Acoust.*, vol. 139, no. 4, p. 40908, May 2017.
- [11] Y. Linzon, B. Ilic, S. Lulinsky, and S. Krylov, "Efficient parametric excitation of silicon-on-insulator microcantilever beams by fringing electrostatic fields," *J. Appl. Phys.*, vol. 113, no. 16, p. 163508, 2013.
- [12] Z. Tang, S. Fan, and C. Cai, "A silicon micromachined resonant pressure sensor," *J. Phys. Conf. Ser.*, vol. 188, no. 1, p. 12042, Sep. 2009.
- [13] S. P. Timoshenko and S. Woinowsky-Krieger, *Theory of plates and shells*. McGraw-hill, 1959.